Inorg. Chem. **2002**, *41*, 577–581

Synthesis, Structure, and Theoretical Study of the Nonclassical $[CuTe_7]^{3-}$ Anion

Perumal Sekar, Frederick P. Arnold, Jr., and James A. Ibers*

Department of Chemistry, Northwestern University, 2145 Sheridan Road, Evanston, Illinois 60208-3113

Received October 22, 2001

The compound $[PPh_4]_2[NEt_4][CuTe_7]$ has been synthesized from the reaction of CuCl with a polytelluride solution in dimethylformamide at room temperature. The compound crystallizes with two formula units in the triclinic space group $P\bar{1}$ in a cell with dimensions $a = 8.9507(18)$ Å, $b = 14.714(3)$ Å , and $c = 23.277(5)$ Å and $\alpha = 86.32(3)°$, $\beta = 80.17(3)°$, and $\gamma = 75.63(3)°$ ($T = -120$ °C). Ab initio calculations indicate that the nonclassical $[CuTe_7]^{3-}$ anion is the result of joining Te_3^{2-} and $[CuTe_4]^{1-}$ fragments through donor–acceptor interactions.

Introduction

Although the chemistry of soluble sulfido- and selenidometalates has been widely investigated,[1−11] the known chemistry of corresponding tellurometalates is more limited.[4,5,12−20] Most of the tellurometalates have no sulfur or selenium analogues and have distinct structure types. Examples include $[M(Te_4)_2]^{2-}$ (M = Zn, Cd, Hg, Pd),[14,21] $[M_2Te_{12}]^{4-}$ (M = Cu, Ag),[13,22] $[M_4Te_{12}]^{4-}$ (M = Cd, Hg),[19,23,24] $[Sn_2Te_6]^{4-}$,[25] $[NbTe_{10}]^{3-}$,[26] $[Ni_4Te_{20}]^{4-}$,[27] $[Cr_3(Te_4)_6]^{3-}$,[28] and $[Cr(Te_4)_3]^{3-}$.[29] The syntheses of many of these species relies on polytelluride anions, Te_n^{2-} ($n > 1$), as the primary tellurium source.

The syntheses, structures, and reactivities of the remarkable nonclassical anions $[AuTe_7]^{3-}$,[30,31] $[AgTe_7]^{3-}$,[31,32] $[HgTe_7]^{2-}$,[20,31,32] and $[ZnTe_7]^{2-}$[20] have been reported. These anions possess unusual structures with unprecedented coordination modes. Among these, the $[ZnTe_7]^{2-}$ anion is the least formidable for a theoretical investigation. However, this anion is disordered in the solid state, and thus the details of its geometry are not well defined. Consequently, we have synthesized $[PPh_4]_2[NEt_4][CuTe_7]$. Here, we present its synthesis, structure, and theoretical description.

* Corresponding author. E-mail: ibers@chem.northwestern.edu.

(1) Müller, A.; Diemann, E. *Adv. Inorg. Chem.* **1987**, *31*, 89−122.
(2) Müller, A.; Jaegerman, W.; Enemark, J. H. *Coord. Chem. Rev.* **1982**, *46*, 245−280.
(3) Kolis, J. W. *Coord. Chem. Rev.* **1990**, *105*, 195−219.
(4) Ansari, M. A.; Ibers, J. A. *Coord. Chem. Rev.* **1990**, *100*, 223−266.
(5) Roof, L. C.; Kolis, J. W. *Chem. Rev.* **1993**, *93*, 1037−1080.
(6) Ansari, M. A.; Ibers, J. A. *Inorg. Chem.* **1989**, *28*, 4068−4069.
(7) McConnachie, J. M.; Ansari, M. A.; Ibers, J. A. *J. Am. Chem. Soc.* **1991**, *113*, 7078−7079.
(8) Ansari, M. A.; Mahler, C. H.; Chorghade, G. S.; Lu, Y.-J.; Ibers, J. A. *Inorg. Chem.* **1990**, *29*, 3832−3839.
(9) McConnachie, J. M.; Ansari, M. A.; Ibers, J. A. *Inorg. Chem.* **1993**, *32*, 3250−3255.
(10) Albrecht-Schmitt, T. E.; Cody, J. A.; Hupp, J. T.; Ibers, J. A. *Inorg. Chem.* **1995**, *34*, 5101−5102.
(11) Albrecht-Schmitt, T. E.; Ibers, J. A. *Inorg. Chem.* **1996**, *35*, 7273−7278.
(12) Ansari, M. A.; McConnachie, J. M.; Ibers, J. A. *Acc. Chem. Res.* **1993**, *26*, 574−578.
(13) Ansari, M. A.; Bollinger, J. C.; Ibers, J. A. *Inorg. Chem.* **1993**, *32*, 1746−1748.
(14) Bollinger, J. C.; Roof, L. C.; Smith, D. M.; McConnachie, J. M.; Ibers, J. A. *Inorg. Chem.* **1995**, *34*, 1430−1434.
(15) McConnachie, J. M.; Bollinger, J. C.; Ibers, J. A. *Inorg. Chem.* **1993**, *32*, 3923−3927.
(16) Kanatzidis, M. G.; Huang, S.-P. *Coord. Chem. Rev.* **1994**, *130*, 509−621.
(17) Dance, I.; Fisher, K. *Prog. Inorg. Chem.* **1994**, *41*, 637−803.
(18) Bollinger, J. C.; Ibers, J. A. *Inorg. Chem.* **1995**, *34*, 1859−1867.
(19) Park, C.-W.; Salm, R. J.; Ibers, J. A. *Can. J. Chem.* **1995**, *73*, 1148−1156.
(20) Müller, U.; Grebe, C.; Neumüller, B.; Schreiner, B.; Dehnicke, K. *Z. Anorg. Allg. Chem.* **1993**, *619*, 500−506.
(21) Adams, R. D.; Wolfe, T. A.; Eichhorn, B. W.; Haushalter, R. C. *Polyhedron* **1989**, *8*, 701−703.
(22) Fenske, D.; Schreiner, B.; Dehnicke, K. *Z. Anorg. Allg. Chem.* **1993**, *619*, 253−260.
(23) Sécheresse, F.; Robert, F.; Marzak, S.; Manoli, J.-M.; Potvin, C. *Inorg. Chim. Acta* **1991**, *182*, 221−228.
(24) Haushalter, R. C. *Angew. Chem., Int. Ed. Engl.* **1985**, *24*, 433−435.
(25) Ansari, M. A.; Bollinger, J. C.; Ibers, J. A. *Inorg. Chem.* **1993**, *32*, 231−232.
(26) Flomer, W. A.; Kolis, J. W. *J. Am. Chem. Soc.* **1988**, *110*, 3682−3683.
(27) McConnachie, J. M.; Ansari, M. A.; Ibers, J. A. *Inorg. Chim. Acta* **1992**, *198*−*200*, 85−93.
(28) Flomer, W. A.; O'Neal, S. C.; Pennington, W. T.; Jeter, D.; Cordes, A. W.; Kolis, J. W. *Angew. Chem., Int. Ed. Engl.* **1988**, *27*, 1702−1703.
(29) Sekar, P.; Ibers, J. A. *Inorg. Chem.* In press.
(30) Ansari, M. A.; Bollinger, J. C.; Ibers, J. A. *J. Am. Chem. Soc.* **1993**, *115*, 3838−3839.
(31) Smith, D. M.; Roof, L. C.; Ansari, M. A.; McConnachie, J. M.; Bollinger, J. C.; Pell, M. A.; Salm, R. J.; Ibers, J. A. *Inorg. Chem.* **1996**, *35*, 4999−5006.
(32) McConnachie, J. M.; Ansari, M. A.; Bollinger, J. C.; Salm, R. J.; Ibers, J. A. *Inorg. Chem.* **1993**, *32*, 3201−3202.

10.1021/ic011092b CCC: $22.00
Published on Web 01/16/2002

Experimental Section

All manipulations were performed under an inert atmosphere of N_2 with the use of standard Schlenk-line techniques or under Ar in a glovebox. Solvents were dried, distilled, and degassed under N_2 before use. Anhydrous *N*,*N*-dimethylformamide (DMF), purchased from Fisher Chemical (Fair Lawn, NJ), was stored over activated molecular sieves and degassed with dry N_2 before use. Anhydrous diethyl ether (Et_2O) and tetrahydrofuran (THF) were distilled from Na/benzophenone. Li_2Te was prepared from the stoichiometric reaction of Li and Te in liquid NH_3. CuCl was purchased from Strem Chemical Co. (Newburyport, MA) and used as received. Energy-dispersive analysis by X-rays (EDAX) was performed with the use of a Hitachi 3500 scanning electron microscope equipped with an X-ray detector. ^{125}Te NMR spectra were obtained on a Varian 400 MHz Unity Plus spectrometer with a 10 mm broadband probe and a deuterium lock. Chemical shifts were referenced to the external standard Ph_2Te_2 at 422 ppm.

Synthesis of $[PPh_4]_2[NEt_4][CuTe_7]$. Li_2Te (250 mg, 1.77 mmol), Te (0.50 g, 3.92 mmol), and NEt_4Cl (165 mg, 1.0 mmol) were dissolved in DMF (10 mL) in a 100 mL Schlenk flask. In another flask, CuCl (99 mg, 1.0 mmol) and PEt_3 (0.2 mL) were added to THF (10 mL), and the mixture was warmed over a water bath until all of the CuCl was digested. This solution was slowly transferred to the polytelluride solution by means of a cannula, and the combined solution was stirred for 1 h. The resulting reddish-purple solution was filtered and treated with a solution of PPh_4Br (838 mg, 2.0 mmol) dissolved in DMF (5 mL), and the mixture was then layered with Et_2O (10 mL). Red-black crystals of $[PPh_4]_2[NEt_4][CuTe_7]$ formed overnight at room temperature. The yield was 852 mg or 59% (based on Te). EDAX performed on several crystals indicated a Cu/Te ratio of 1:7. The compound is extremely air- and moisture-sensitive, and neither satisfactory elemental analyses nor mass spectra could be obtained. ^{125}Te NMR (DMF, δ): −812, −1067. These values are not comparable with those in related compounds and may be from a decomposition product.

Crystallography. Crystals of $[PPh_4]_2[NEt_4][CuTe_7]$ could be handled very briefly when the Schlenk tube was opened under oil. A crystal of dimensions 0.074 mm × 0.076 mm × 0.144 mm was mounted on a glass fiber that was then attached to a goniometer head and placed in the cold stream of the diffractometer. Single-crystal X-ray diffraction data were collected with the program SMART[33] on a Bruker Smart 1000 CCD diffractometer[33] at −120 °C with the use of monochromatized Mo Kα radiation ($\lambda = 0.71073$ Å). The diffracted intensities generated by a scan of 0.3° in ω were recorded on four sets of 606 frames at $\phi = 0$, 90, 180, and 270°, with an additional 50 frames at $\phi = 0°$ for detection of possible decay. The exposure times were 15 s/frame. Cell refinement and data reduction were carried out with the use of the program SAINT.[33] Face-indexed absorption corrections were made with the program XPREP.[34] Then SADABS was employed to make incident-beam and decay corrections.[33] The structure was solved by direct methods with SHELXS and was refined by full-matrix least-squares techniques with SHELXL in the SHELXTL-97 suite.[34] Hydrogen atoms were generated in calculated positions and constrained with the use of a riding model. The final model involved anisotropic displacement parameters for all non-hydrogen atoms. Crystallographic data are listed in Table 1, and selected bond distances and angles are listed in Table 2. Additional information is available in the Supporting Information.

Table 1. Crystallographic Data for $[PPh_4]_2[NEt_4][CuTe_7]$

formula	$C_{56}H_{60}CuNP_2Te_7$
fw	1765.73
space group	$P\bar{1}$
a (Å)	8.9507(18)
b (Å)	14.714(3)
c (Å)	23.277(5)
α (deg)	86.32(3)
β (deg)	80.17(3)
γ (deg)	75.63(3)
V (Å^3)	2925.3(10)
Z	2
T (°C)	−120
ρ_{calcd} (g/cm^3)	2.005
μ(Mo Kα) (mm^{-1})	38.85
$R_1(F)^a$	0.040
$R_w(F^2)^b$	0.074

[a] $R_1(F) = \Sigma||F_o| - |F_c||/\Sigma|F_o|$. [b] $R_w(F_o^2) = [\Sigma\, w(F_o^2 - F_c^2)^2/\Sigma\, wF_o^4]^{1/2}$; $w^{-1} = \sigma^2(F_o^2) + (0.04F_o^2)^2$ for $F_o^2 > 0$; $w^{-1} = \sigma^2(F_o^2)$ for $F_o^2 \le 0$.

Table 2. Selected Bond Distances and Angles for the Anions of $[PPh_4]_2[NEt_4][CuTe_7]^a$, $[PPh_4]_2[NEt_4][AgTe_7]^b$, $[K(15\text{-Crown-}5]_2[HgTe_7]^c$, $[PPh_4]_2[HgTe_7]^b$, and $[NEt_4]_2[HgTe_7]^b$

M	Cu[a]	Ag[b]	Hg[c]	Hg[b,d]	Hg[b,e]
			Bond Distances (Å)		
M−Te(1)	2.518(1)	2.702(2)	2.710(3)	2.730(2)	2.715(2)
M−Te(4)	2.532(1)	2.725(2)	2.681(3)	2.742(1)	2.718(2)
M−Te(7)	2.505(1)	2.695(2)	2.681(3)	2.722(2)	2.719(2)
Te(1)−Te(2)	2.766(1)	2.756(2)	2.588(5)	2.746(2)	2.754(2)
Te(2)−Te(3)	2.717(1)	2.714(2)	2.657(9)	2.716(2)	2.713(2)
Te(3)−Te(4)	3.225(1)	3.230(2)	3.258(8)	2.997(2)	3.008(2)
Te(4)−Te(5)	2.894(1)	2.866(2)	2.962(4)	3.050(2)	3.039(2)
Te(5)−Te(6)	2.725(1)	2.720(2)	2.666(3)	2.682(2)	2.721(2)
Te(6)−Te(7)	2.733(1)	2.721(2)	2.962(4)	2.727(2)	2.742(2)
			Bond Angles (deg)		
Te(1)−M−Te(4)	127.34(3)	124.48(6)	117.8(1)	117.70(5)	118.32(5)
Te(1)−M−Te(7)	112.89(4)	119.45(6)	117.8(1)	124.37(5)	121.93(4)
Te(4)−M−Te(7)	119.77(4)	116.07(6)	124.3(1)	117.92(4)	119.74(5)
M−Te(1)−Te(2)	102.18(3)	99.48(5)	101.9(1)	95.97(5)	94.65(5)
M−Te(4)−Te(3)	90.82(3)	89.41(5)	90.3(1)	92.75(4)	93.43(5)
M−Te(4)−Te(5)	96.34(3)	95.52(5)	96.4(1)	90.53(6)	92.34(5)
M−Te(7)−Te(6)	99.99(4)	96.89(6)	96.4(1)	96.72(4)	96.71(5)
Te(1)−Te(2)−Te(3)	102.97(4)	105.21(5)	101.7(3)	100.83(4)	101.59(5)
Te(2)−Te(3)−Te(4)	105.07(3)	106.69(5)	101.9(1)	101.66(5)	100.47(5)
Te(3)−Te(4)−Te(5)	172.16(2)	174.12(5)	173.3(2)	174.52(5)	170.40(5)
Te(4)−Te(5)−Te(6)	101.23(3)	102.15(5)	109.2(1)	102.04(5)	104.57(5)
Te(5)−Te(6)−Te(7)	99.77(3)	101.84(5)	109.2(1)	102.50(5)	101.91(6)

[a] Present work. [b] References 31 and 32. [c] Reference 20. [d] PPh_4^+. [e] NEt_4^+.

Computational Details. All calculations on the $[CuTe_7]^{3-}$ anion were performed with the ab initio electronic structure package GAMESS.[35] For the geometry optimization, the Hessian calculation, and the natural bond order (NBO) analysis, the effective core potential and associated valence basis set of Stevens and co-workers were used,[36−38] with additional d ($z = 0.237$) and sp ($z = 0.0306$) functions augmenting the Te basis set. The geometry was optimized at the second-order Moller−Plesset (MP2)[39,40] frozen-core (MP2-

(33) SMART version 5.054 data collection and SAINT-Plus version 6.02A data processing software for the SMART system; Bruker Analytical X-ray Instruments, Inc., Madison, WI, 2000.

(34) Sheldrick, G. M. SHELXTL DOS/Windows/NT version 5.10; Bruker Analytical X-ray Instruments, Inc., Madison, WI, 1997.

(35) Schmidt, M. W.; Baldridge, K. K.; Boatz, J. A.; Elbert, S. T.; Gordon, M. S.; Jensen, J. H.; Koseki, S.; Matsunaga, N.; Nguyen, K. A.; Su, S.; Windus, T. L.; Dupuis, M.; Montgomery, J. A., Jr. *J. Comput. Chem.* **1993**, *14*, 1347−1363.

(36) Stevens, W. J.; Basch, H.; Krauss, M. *J. Chem. Phys.* **1984**, *81*, 6026−6033.

(37) Stevens, W. J.; Krauss, M.; Basch, H.; Jasien, P. G. *Can. J. Chem.* **1992**, *70*, 612−630.

(38) Cundari, T. R.; Stevens, W. J. *J. Chem. Phys.* **1993**, *98*, 5555−5565.

(39) Pople, J. A.; Binkley, J. S.; Seeger, R. *Int. J. Quantum Chem., Symp.* **1976**, *10*, 1−19.

(40) Frisch, M. J.; Head-Gordon, M.; Pople, J. A. *Chem. Phys. Lett.* **1990**, *166*, 275−280.

(FC)) level of theory, with the Cu 3s and 3p orbitals considered to be core orbitals. The optimized geometry was verified to be a minimum-energy structure because the Hessian possessed no negative eigenvalues. The molecule was initially optimized at the restricted Hartree−Fock (RHF) level of theory with no symmetry constraints; however, because the resulting structure was symmetric to within 0.0001 Å, the structure was symmetrized to C_2 symmetry to facilitate the MP2 calculations. The Hessian was calculated numerically by double-differencing.

The resulting wave function of the MP2 optimized structure was analyzed with the use of NBO 4.0 m,[41] within the NBO and natural localized molecular orbital (NLMO)[42] approximations, at both the RHF and MP2 levels of theory. The bond orders were calculated with the use of the NLMO approximation[42] because this method is consistent with the methodology used to describe the bonding.

Synthesis and Structure

Synthesis. The $[MTe_7]^{n-}$ anions have no Se or S analogues. $[PPh_4]_2[NEt_4][CuTe_7]$ was synthesized from the reaction of CuCl with polytelluride anions in DMF at room temperature, in the presence of PEt_3 and NEt_4Cl, followed by the addition of PPh_4Br. The phosphine increases the solubility of CuCl and also provides the basic medium for the reaction. However, note that $[PPh_4]_2[Hg(Te_4)_2]$[14] and $[PPh_4]_2[HgTe_7]$[31,32] were previously synthesized from the reaction of $Hg(xanthate)_2$ or $HgCl_2$ in DMF with or without the addition of PEt_3. The Ag analogue $[PPh_4]_2[NEt_4][AgTe_7]$[31,32] was prepared previously in the present manner, except for the addition of Na. Because $[PPh_4]_2[NEt_4][CuTe_7]$ can be obtained from the above reaction with or without addition of Na, formation of $[CuTe_7]^{3-}$ may result from the presence of the mixed countercations (PPh_4^+ and NEt_4^+) and not from the addition of Na, as proposed for the formation of $[PPh_4]_2[NEt_4][AgTe_7]$.[31] Note that $[NEt_4]_4[(Te_4Cu)(\mu\text{-}Te_4)(CuTe_4)]$ was obtained previously from the same reaction when PPh_4Br was omitted.[13] However, the formation of the related anion $[HgTe_7]^{2-}$ does not depend on the cation because it has been isolated with three different countercations.[20,31,32] Cation size does play an important role in the isolation of some tellurometalates. For example, $[Au_2Te_4]^{2-}$ is isolated with the PPN^+,[43] PPh_4^+,[44] and NPr^+ [45] cations, but $[AuTe_7]^{3-}$, which has a different structure from that of $[CuTe_7]^{3-}$, is isolated from the same medium with the NEt_4^+ cation.[30,31]

Structural Description. The structure of $[PPh_4]_2[NEt_4][CuTe_7]$ consists of well-separated cations and anions. The structure of the $[CuTe_7]^{3-}$ anion (Figure 1) is very similar to the structures of the $[AgTe_7]^{3-}$ [31,32] and $[HgTe_7]^{2-}$ anions.[20,31,32] The $[CuTe_7]^{3-}$ anion contains a Cu(I) center coordinated in a trigonal planar fashion to three Te atoms of what is formally an η^3-Te_7^{4-} ligand. The central Te(4) atom of the η^3-Te_7^{4-} ligand is coordinated to the Cu atom and to the Te(3) and Te(5) atoms in a "T"-shaped geometry. The Cu, Te(1), Te(3), Te(4), Te(5), Te(7) portion of the anion is nearly planar, with the average deviation from the least-squares plane being 0.11 Å. Atoms Te(2) and Te(6) deviate from this plane in opposite directions by 1.01 and 1.27 Å, respectively. Generally, the metrical data for the $[MTe_7]^{n-}$ anions (Table 2) are comparable, with Cu−Te distances being shorter than Ag−Te or Hg−Te distances. The three Cu−Te distances, 2.505(10), 2.518(11), and 2.532(10) Å, may be compared to those of 2.492(4)−2.514(4) Å in $[NEt_4]_4[Cu_2Te_{12}]$.[13]

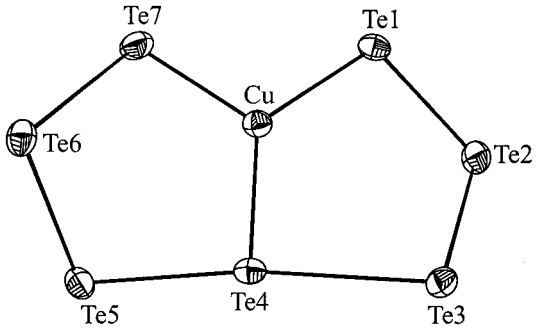

Figure 1. Molecular structure of the $[CuTe_7]^{3-}$ anion with the 50% probability displacement ellipsoids shown.

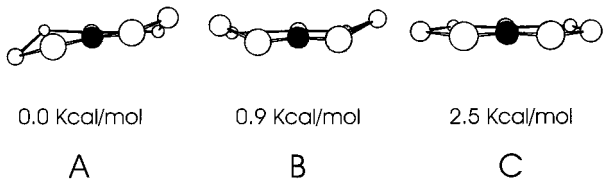

Figure 2. Relative energies of the $[CuTe_7]^{3-}$ anion in C_2 (A), C_s (B), and C_{2v} (C) symmetry. The view is down the Cu−Te(4) axis. The Cu atom is filled and at the center of each structure, and the Te atoms are open.

Table 3. Calculated and Experimental Bond Distances

bond	calcd (Å)[a]	exp (Å)	expt av[a]
Cu−Te(4)	2.554	2.532(1)	2.532
Cu−Te(1)	2.560	2.518(1), 2.505(1)	2.512
Te(4)−Te(5)	3.093	3.225(1), 2.894(1)	3.060
Te(2)−Te(3)	2.816	2.717(1), 2.725(1)	2.721
Te(1)−Te(2)	2.837	2.766(1), 2.733(1)	2.750

[a] C_2 symmetry.

Of particular interest is the Te3−Te4−Te5 interaction in these compounds. In all cases (Table 2), this interaction is essentially linear; it is unsymmetric in the Cu, Ag, and one Hg compound, but it is symmetric in the other two Hg compounds. This point is discussed below.

Theoretical Results

Geometry. Three trial geometries considered for the $[CuTe_7]^{3-}$ anion are shown in Figure 2. The C_s structure (B) was determined to be a transition state lying approximately 0.9 kcal/mol above the C_2 (A) minimum. The planar C_{2v} structure (C) was slightly higher in energy (2.5 kcal/mol). It possesses three negative eigenvalues, indicating that it is neither a minimum nor a saddle point on the potential energy surface; therefore, it is of no interest chemically. Selected bond lengths for the calculated minimum-energy C_2 structure are shown in Table 3. These generally agree to better than 0.1 Å with the average experimental values.

The calculated structure of the $[CuTe_7]^{3-}$ anion possesses C_2 symmetry, but experimentally, the Te(3)−Te(4)−Te(5) interaction is unsymmetric. The energy involved in this distortion was calculated by varying the Te(4)−Te(5) bond length in 0.1 Å increments while freezing the positions of all other atoms. As may be seen in Figure 3, a contraction of the bond from 3.09 (the calculated equilibrium distance) to 2.89 Å costs <2 kcal/mol, whereas lengthening it to 3.19

(41) *NBO 4.M Program Manual*; Weinhold, F., Ed.; University of Wisconsin: Madison, Wisconsin, 1999.
(42) Reed, A. E.; Weinhold, F. *J. Chem. Phys.* **1985**, *83*, 1736−1740.
(43) Haushalter, R. C. *Inorg. Chim. Acta* **1985**, *102*, L37−L38.
(44) Warren, C. J.; Ho, D. M.; Bocarsly, A. B.; Haushalter, R. C. *J. Am. Chem. Soc.* **1993**, *115*, 6416−6417.
(45) Dhingra, S. S.; Haushalter, R. C. *Inorg. Chem.* **1994**, *33*, 2735−2737.

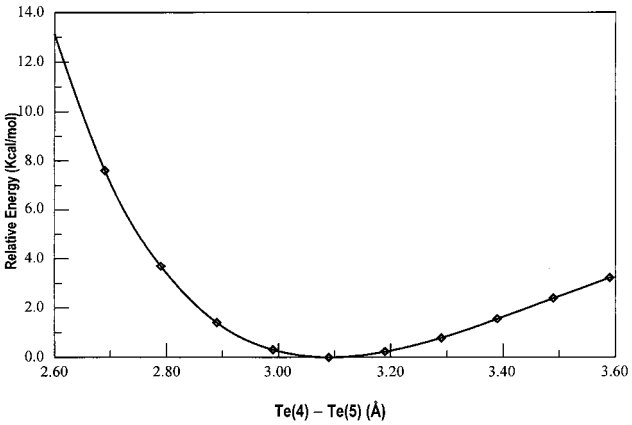

Figure 3. Change in energy (kcal/mol) caused by distortion of the Te(4)−Te(5) bond by ±0.5 Å in the $[CuTe_7]^{3-}$ anion.

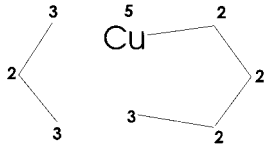

Figure 4. Classical Lewis bonding pattern. The number of lone pairs per atomic center is shown.

Å costs <1 kcal/mol. Similar results are found for the $[HgTe_7]^{2-}$ system, where a distortion of 0.3 Å costs ∼5 kcal/mol, and for the $[AuTe_7]^{3-}$ system, where the experimentally determined structure that is significantly distorted from the common MTe_7 framework is found to lie <5 kcal/mol lower in energy.[46] We therefore ascribe the experimentally observed distortions from ideal C_2 structure to packing forces arising from the positions of the cations. The fact that the symmetry of the Te(3)−Te(4)−Te(5) interaction in the $[HgTe_7]^{2-}$ anion is cation-dependent, being unsymmetric in $[K(15\text{-crown-}5]_2[HgTe_7]$[20] but essentially symmetric in $[PPh_4]_2[HgTe_7]$ and $[NEt_4]_2[HgTe_7]$,[31,32] adds credence to this explanation.

Electronic Structure. It is easier to discuss the electronic structure of the $[CuTe_7]^{3-}$ anion if we begin with the limiting case of a classical Lewis structure. There are 28 valence-electron pairs in $[CuTe_7]^{3-}$. If we start with the presumption that each Te atom possesses two pairs, then 14 pairs are accounted for. Each Te−Te or Te−Cu bond accounts for another pair, which amounts to another eight pairs given the starting structure shown in Figure 4. In this first-order description, atom Te(2) is bonded to atoms Te(3) and Te(4) and possesses two lone pairs. We assume that Te(2) is not bonded to the Cu atom. Thus, six pairs remain unaccounted for but are assumed to reside on the Cu atom. From an electron-counting standpoint, this situation leads to the requirement of a Cu(−III) center. If we break one of the Cu−Te bonds, then one Te atom has one bond and three lone pairs (eight electrons), and the Cu atom has the remaining six pairs, bringing the count down to Cu(−I). If we break one of the Te−Te bonds and then divide one of the electron pairs from the Cu atom between the Te atoms to close the valences, then the Cu atom formally becomes the known Cu(I), and a dianionic pure-Te fragment and a Cu-containing monoanionic fragment result (Figure 4).

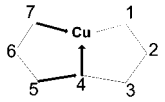

Figure 5. NBO-derived bonding pattern. Arrows indicate donor−acceptor interactions, whereas solid lines indicate traditional covalent and ionic bonds.

Table 4. Atomic Charges by Natural Population Analysis of the Symmetry-Unique Atoms

atom	RHF	MP2
Cu	0.62	0.48
Te(4)	−0.57	−0.64
Te(3)	−0.51	−0.47
Te(1)	−0.71	−0.69
Te(2)	−0.30	−0.27

The system was analyzed in terms of two-center bonds and then was relaxed to allow three-center bonds to form. In the end, the description involving only two-center contributions had a higher percentage (99.74%) of electrons in the Lewis configuration than did the more delocalized three-center description (99.26%). Therefore, only the NBO analysis based on two-center bonds will be discussed. Within this description, the Cu has an electronic configuration of $4s^{0.5}3d^{9.8}$, which would be rounded up formally to $4s^{1}3d^{10}$, although arguments in favor of $4s^{0}3d^{10}$ could also be made on chemical grounds. The ambiguity persists in the atomic charges, with the RHF descriptions giving a charge of 0.62 on Cu and the correlated description decreasing that value to 0.48 (Table 4).

The resulting structure is shown in Figure 5 in which the $[CuTe_7]^{3-}$ ion has been broken into Te_3 and $CuTe_4$ fragments, with each fragment carrying a −1.5 charge. There exists no Te(4)−Cu bond in the first-order description. Each terminal Te atom (Te(7), Te(5), Te(4)) has three lone pairs present. This situation is sterically undesirable, and second-order corrections indicate that donations of charge from Te lone pairs to Cu vacant orbitals and to (Cu,Te)−Te antibonding orbitals stabilize the structure and join the two fragments. These delocalizations are best seen through the NLMO analysis, which again indicates that the base framework includes the Te(7)−Te(6)−Te(5) and the Cu−Te(1)−Te(2)−Te(3)−Te(4) fragments. The various electron pairs on the Cu atom are all >99% localized on the metal center. Atom Te(4) has a lone pair that is 91% localized on Te(4) but is delocalized onto Cu by approximately 7%, with the balance being delocalization "tails" that interact with the Cu−Te(1) antibonding orbital and with the other neighboring Te centers. Similarly, atom Te(5) has an orbital that is delocalized 15% onto atom Te(4) and 4% into the Te(4)−Te(3) antibonding orbital. Atom Te(7) has a delocalization tail of 5% onto Cu and 1% onto Te(6). These donor−acceptor interactions weaken the primary bonds but create the C_2 structure with two closed rings, as seen in Figure 2. Because only on the Cu atom are there unoccupied orbitals, most of the delocalization tails involve interactions with Te−Te antibonding orbitals, which are identified through the second-order perturbation of the NBO analysis. The weak Te(3)−Te(4) bond arises from the donation of lone pairs on Te(5) into

(46) Arnold, F. P., Jr. Unpublished results.

Table 5. Selected Antibonding Populations

antibonding orbital	RHF	MP2
Cu−Te(1)	0.24	0.32
Te(4)−Te(3)	0.38	0.52
Te(5)−Te(6)	0.06	0.14
Te(7)−Te(6)	0.05	0.16
Te(3)−Te(2)	0.08	0.17
Te(1)−Te(2)	0.08	0.21
total no. of electrons	0.89	1.52

Table 6. NLMO Bond Orders

bond	RHF	MP2
Cu−Te(1)	0.13	0.17
Cu−Te(4)	0.14	0.20
Cu−Te(7)	0.13	0.17
Te(4)−Te(3)	0.30	0.32
Te(4)−Te(5)	0.38	0.46
Te(3)−Te(2)	0.86	0.94
Te(5)−Te(6)	0.86	0.91
Te(7)−Te(6)	0.83	0.89
Te(1)−Te(2)	0.82	0.93

the Te(4)−Te(3) antibonding orbitals. Similarly, donation from Te(7) weakens the Cu−Te(1) bond, whereas the lone pairs on Te(4) interact with both vacant orbitals on Cu of Rydberg character and more strongly with the Cu−Te(1) antibonding orbital.

These delocalizations result in significant electron populations in the antibonding orbitals, as shown in Table 5. At the RHF level of theory, these orbitals are primarily the Cu−Te(1) and the Te(3)−Te(4) antibonding orbitals. The inclusion of correlation (MP2) increases the degree of delocalization, causes a significant contribution into the remaining Te−Te antibonding orbitals, and raises the net antibonding population from 0.89 to 1.52 electrons. The lone-pair populations on the various Te centers are ≥1.92 at both the RHF and MP2 levels of theory. Correspondingly, the bond orders (Table 6) are therefore rather low for those bonds involving either Cu or Te(4), being approximately one-half the value of the Te−Te bonds in the bent Te_3 units. The low RHF bond orders are to be expected because RHF overestimates the ionic character of the system;[47,48] therefore, the electrons are more localized on the atomic centers. Thus, we generally find that the bond orders calculated at the MP2 level of theory are higher by 0.02−0.08 for those bonds involving Cu or Te(4). These changes are very small, indicating that the primary bonding orbitals are little affected by the addition of correlation. From the resulting bond orders, one might infer that the system could alternatively be described as a pair of Te_3 units, a free Cu, and a free Te atom, but this is an artifact that results from considering only one of the symmetry-equivalent pairs of structures. The NBO structure presumes, for instance, that there is a covalent Te(4)−Te(3) bond and a donor−acceptor interaction between Te(5) and Te(4). By symmetry, there is also a configuration in which there is a covalent Te(5)−Te(4) bond and a donor−acceptor interaction between Te(4) and Te(3). These two structures average to the results that would be drawn from the NLMO bond orders alone and therefore do not contradict the structure suggested by the parent NBO analysis plus the associated delocalizations.

We therefore conclude that the observed structure is the result of joining a Te_3^{2-} fragment with a $[CuTe_4]^{1-}$ fragment through donor−acceptor interactions. The structure is heavily stabilized by delocalizing the third lone pairs from Te(4), Te(7), and Te(5) into the p-type acceptor orbitals on Cu and, owing to charge capacity effects at Cu, into the antibonding orbitals of the σ-framework.[49,50] This delocalization leads to a weakening of the Te−Te and Cu−Te bonds and to a structure that is easily distorted in the solid state. The good agreement between the calculated and crystallographically determined structures of the anion indicates that despite the high charge on the free anion, very little of this charge is transferred to the counterions in the solid state. We therefore expect the destabilizing effects to be mitigated in the heavier Au and Hg systems because of the greater ability of the third-row metals to accommodate the excess charge in the system, thereby resulting in stronger M−Te and Te−Te bonds.

Acknowledgment. This work was supported by the National Science Foundation (Grant no. CHE-9819385).

Supporting Information Available: Crystallographic data in CIF format for $[PPh_4]_2[NEt_4][CuTe_7]$. This material is available free of charge via the Internet at http://pubs.acs.org.

IC011092B

(47) Veillard, A. *Chem. Rev.* **1991**, *91*, 743−766.
(48) Benson, M. T.; Cundari, T. R.; Lim, S. J.; Nguyen, H. D.; Pierce-Beaver, K. *J. Am. Chem. Soc.* **1994**, *116*, 3955−3966.
(49) Politzer, P. *J. Chem. Phys.* **1986**, *86*, 1072−1073.
(50) Brinck, T.; Murray, J. S.; Politzer, P. *Inorg. Chem.* **1993**, *32*, 2622−2625.